Formation of a new crystalline qtz-[Zn(mIm)$_2$] polymorph from amorphous ZIF-8

Michael F. Thorne,[‡a] Celia Castillo-Blas,[‡a] Lauren N. McHugh,[a] Alice M. Bumstead,[a] Georgina Robertson,[a] Adam F. Sapnik,[a] Chloe S. Coates,[b] Farheen N. Sayed,[b] Clare P. Grey,[b] David A. Keen,[c] Martin Etter,[d] Ivan da Silva,[c] Krunoslav Užarević,[e] and Thomas D. Bennett [a*]

Materials

Zinc nitrate hexahydrate (99 %), and methanol (HPLC grade) were purchased from Fisher scientific. 2-methylimidazole (99 %), DMSO-d$_6$ (0.03 % TMS), D$_2$O (35 % DCl) were purchased from Sigma Aldrich. Methylene Blue trihydrate was purchased from ACROS organics. All materials were used as received with no further purification.

Methods

Synthetic procedure for SOD-ZIF-8

Firstly, a solution of zinc nitrate hexahydrate 2.933 g (9.78 mmol) in methanol (200 mL) was prepared. Also, a solution of 2-methylimidazole 6.489 g (79.04 mmol) in methanol (200 mL) was prepared. The 2-mIm solution was stirred, and the zinc nitrate solution was poured into the 2-mIm solution. The resulting solution was stirred for 1 hour directly after mixing. The cloudy suspension was transferred into centrifuge tubes (40 mL per tube, 10 tubes) and centrifuged at 4000 RPM for 10 minutes. After this the ZIF-8 white powder was deposited at the bottom of the centrifuge tube. The excess methanol was discarded, and fresh methanol (20 mL per tube) was added. The ZIF-8 particles were re-dispersed by mixing and re-centrifuged at 4000 RPM for 10 minutes. After this, the solid was collected and heated to 40 °C overnight.

Amorphisation for ZIF-8

SOD-ZIF-8 (200 mg) was added to a 10 mL stainless steel ball mill jar, along with 1 x 10 mm stainless steel ball (4.03 g) and milled for 60 minutes at 20 Hz in a Retsch MM 400 mixer mill.

Formation of qtz-[Zn(mIm)$_2$]

a$_m$ZIF-8 (10-20 mg) was added to an aluminium DSC pan and heated to 400 °C at 10 ° C min^{-1} under an argon atmosphere in a Netsch 214 Polyma DSC. The synthesis of this material under vacuum or N$_2$ flow was, however, unsuccessful.

Thermogravimetric analysis (TGA)

TGA was performed on a TA Q600 under an argon atmosphere with a heating rate of 10 °C min^{-1}, 5-15 mg of activated sample was used in each run.

Differential scanning calorimetry (DSC)

DSC was performed on a Netsch 214 Polyma. A background correction scan, sapphire standard scan and sample scan were performed to obtain a heat capacity trace.

The DIN 51007 method was used to obtain the heat capacity trace from the sapphire and sample trace. For this an isothermal treatment at 30 °C was performed for 5 minutes, then a heating scan at 10 °C min^{-1} to 400 °C was performed, followed by a 5-minute isothermal treatment at 400 °C all under an argon atmosphere. This heating profile was performed on the sample, background correction, and sapphire standard.

DSC experiments on **qtz**-[Zn(mIm)$_2$] were performed by isothermally treating at 30 °C, then heating to 450 °C at 10 C min^{-1}, followed by a 5-minute isothermal treatment at 450 °C. Next, a cooling step to 30 °C at 10 C min^{-1} was performed. This was then repeated to give a second heating/cooling scan. All scans were performed under an argon atmosphere.

Powder X-ray Diffraction (PXRD)

PXRD was performed on a Bruker D8 Advance using Cu Kα radiation (λ = 1.5418 Å), between 5–40 2θ° at room temperature.

PXRD of **qtz**-[Zn(mIm)$_2$] was collected using a Bruker D8-advance diffractometer using Cu Kα (λ = 1.5418 Å) radiation and a LynxEye position sensitive detector in reflectance Bragg-Brentano geometry employing. A 5-80° 2θ angular range was used with a step size of 0.01° and a step time of 1.5 s.

Synchrotron *in-situ* milling powder X-ray diffraction

The *in-situ* ball milling PXRD experiments were performed at the Deutsches Elektronen synchrotron (DESY), Hamburg at PETRA III beamline P02.1. The beam size was *ca*. 1 x 1 mm^2 and λ = 0.20735 ± 0.00001 Å (59.79321 ± 0.00159 keV). The beamline was equipped with a Varex XRD4343CT detector and modified vibratory ball mill. Beam alignment and calibration was performed using a Si standard in a PMMA milling jar. To avoid having two sample positions (*i.e.* sample on both sides of the PMMA jar), the beam was aligned with the bottom of the PMMA jar. Data was processed by removing the amorphous background contributed by PMMA.

For the amorphisation of ZIF-8, evacuated ZIF-8 (200 mg) was added to a 10 mL PMMA ball mill jar, along with 1 x 10 mm stainless steel ball (4.03 g) and milled for 60 minutes at 20 Hz.

Synchrotron powder X-ray diffraction

The diffraction data used for the Rietveld refinement of the structure of the **qtz**-[Zn(mIm)$_2$] material was collected at Diamond Light Source (beamline I11, λ= 0.82697 Å) using a 0.5 mm glass capillary and a Mython2 Position Sensitive Detector (PSD), at room temperature.

CHN Microanalysis

CHN combustion analysis was performed using a CE440 Elemental Analyser, EAI Exeter Analytical Inc. ∼2 mg of sample was used for each run to give C%, H% and N% values.

Scanning Electron Microscopy (SEM)

SEM was performed using a FEI Nova NanoSEM operated at 5 keV for imaging using secondary electron signal. Samples were prepared for SEM by securing to aluminium SEM pin stubs using carbon tape. Samples were coated in palladium using an Emtech K575 sputter coater prior to imaging.

^{1}H Nuclear Magnetic Resonance Spectroscopy (^{1}H NMR)

^{1}H NMR samples were prepared by digesting the ZIF (5–10 mg) in a solution of DMSO-d_6 (1.0 mL, 0.03% TMS), D_2O (0.2 mL, 35% DCl). Glass samples required sonication for 5 minutes to allow for complete dissolution. Samples were run in a Bruker Advance III HD 500 MHz spectrometer. Spectra were calibrated using TMS as a standard.

Fourier Transformed Infrared Spectra (FTIR)

IR spectra were collected from KBr pellets using a Bruker Tensor 27 FTIR spectrometer in transmission mode between 550 and 4000 cm^{-1}. Pellets were prepared dispersing a small amount of powder samples in KBr using a pellet press at 10 tons for 10 minutes and a 13 mm of diameter pellet dye. A background was subtracted from all spectra prior to analysis from a pristine KBr pellet.

Methylene blue absorption

Firstly, a stock aqueous methylene blue (MB) solution (5 mg in 100 mL distilled water) was prepared. 10 mg of activated sample was added to 10 mL dye solution. The resulting suspensions were stirred for 48 hours, after which the solid ZIF powders were removed *via* filtration yielding aqueous MB to be examined using UV-VIS spectroscopy.

Ultraviolet–visible spectroscopy (UV-*VIS*)

UV-Vis experiments were performed using an Agilent UV-Vis spectrophotometer, in the range 190 – 1100 nm. Samples were measured in rectangular polystyrene cuvettes with a path-length of 10 mm, and a total volume of 3.5 mL.

Firstly, a calibration curve for aqueous MB was performed by producing 5, 4, 3, 2, 1, 0.5 and 0.025 mg L^{-1} solutions of MB in distilled water. These solutions, along with a distilled water blank, were measured to produce a range of absorbances for aqueous MB. The MB absorbance at 665 nm was used for producing the calibration curve.

Next the ZIF-8, a$_m$ZIF-8 and **qtz**-[Zn(mIm)$_2$] filtered MB solutions were measured. The solutions were diluted by a factor of 10 to allow for absorbances lower than 1.0. The absorbance for the 665 nm peak from these solutions were then compared to the calibration curve. From this the amount of MB remaining in each solution was determined, and a percentage extraction (when compared to the starting stock solution) was calculated.

Supplementary Data

Powder Refinement: Rwp = 5.46%   Rwp(w/o bck) = 9.58%   Rp = 3.97%
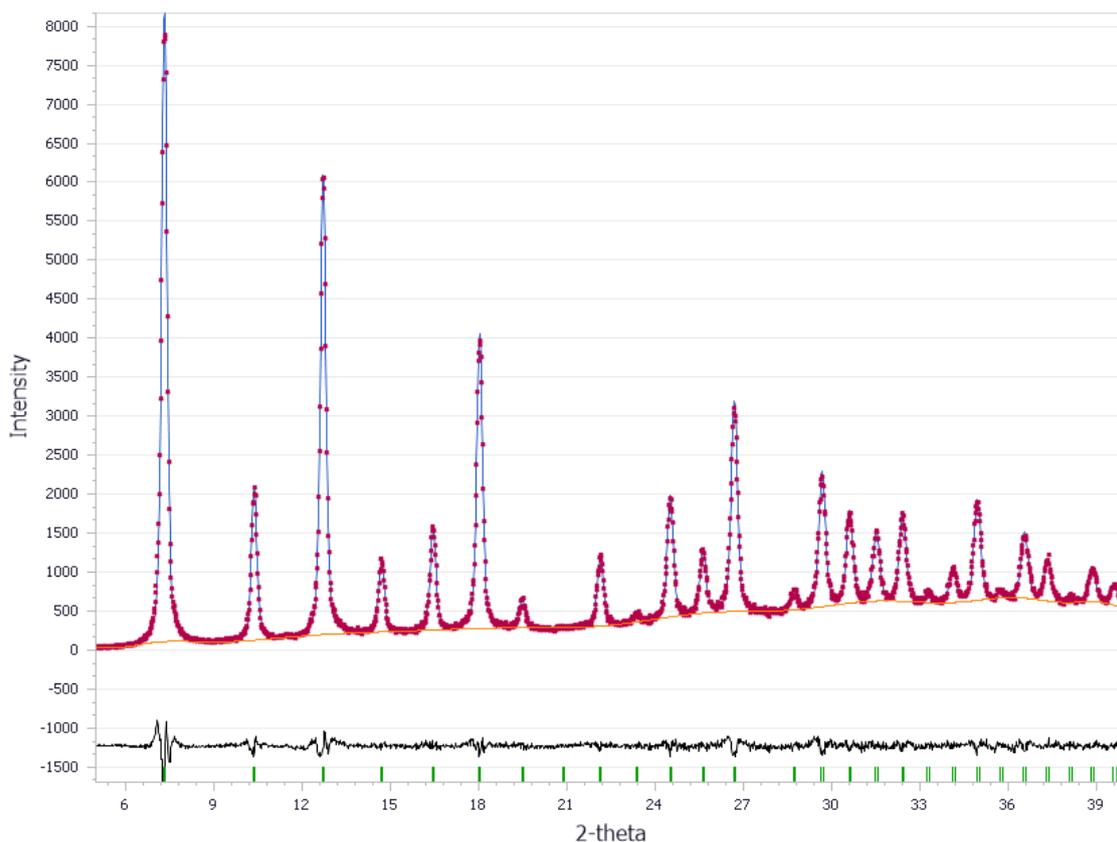
Figure S1: Pawley refinement of ZIF-8 against a literature CIF using space group *I-43m* (λ = 1.5406 Å).[1] Experimental results (red), simulated diffraction pattern (blue), background (orange) and difference pattern (black), tick marks of hkl values (green).

Table S1: Pawley refinement details of ZIF-8

R_{wp}	Space Group	Lattice Parameters	Lattice Parameters Reported for ZIF-8
5.46 %	*I-43m*	a = 17.0986 (17) Å	a = 16.9910(12) Å
		α = 90 °	α = 90 °
		β = 90 °	β = 90 °
		γ = 90 °	γ = 90 °

4
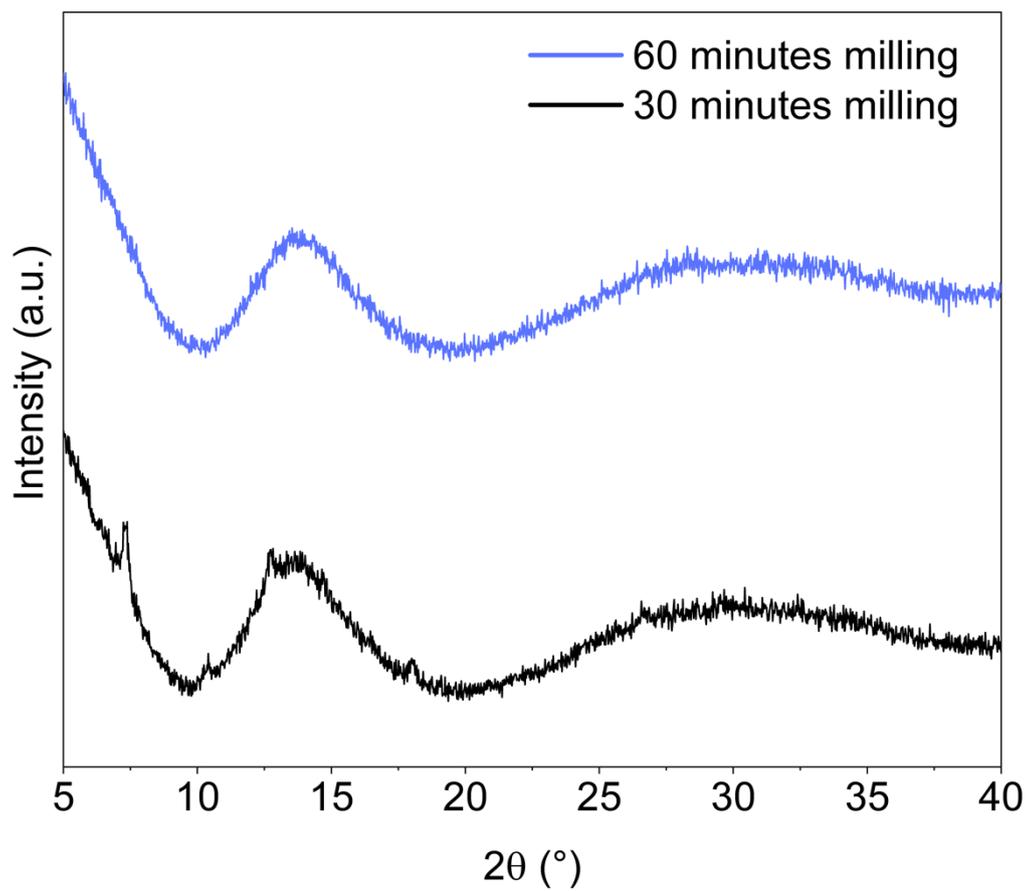
Figure S2: Ball-milled amorphisation of **SOD**-ZIF-8 showing small residual Bragg peaks (λ = 1.5406 Å) after 30 minutes, and complete amorphisation after 60 minutes of mechanical ball-mill.
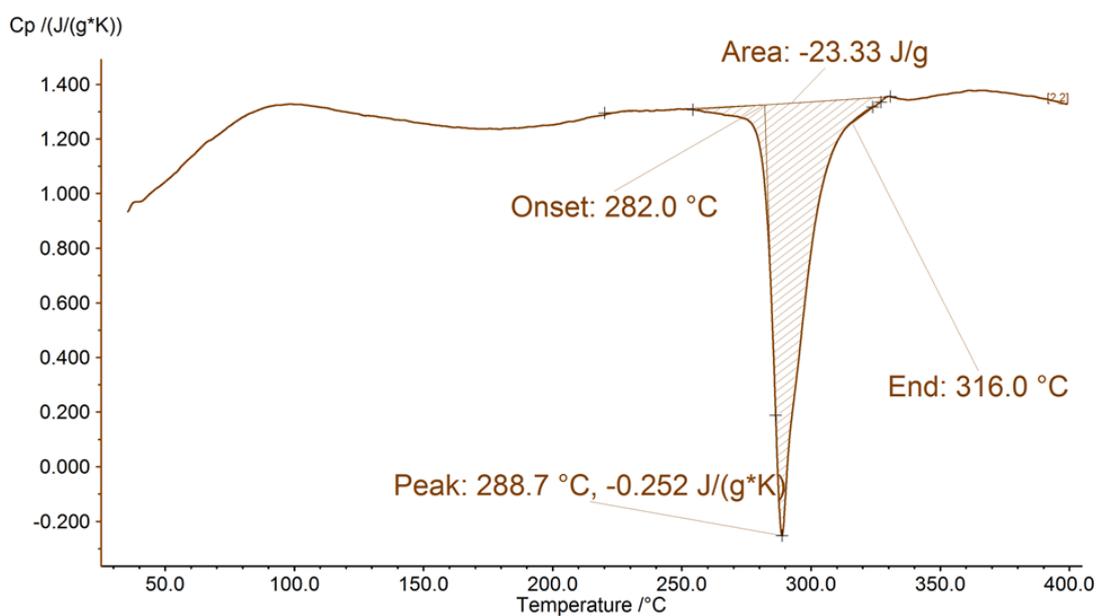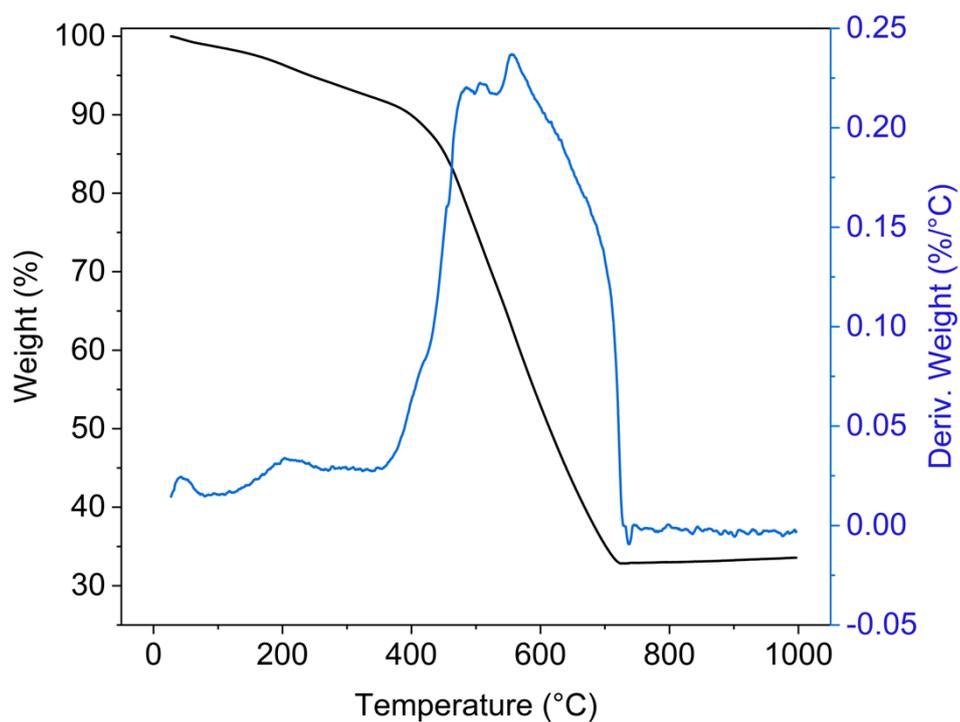
Figure S3: (Top) Full TGA of a_mZIF-8 performed at 10 °C min^{-1} under an argon atmosphere showing major onset of decomposition over 400 °C; (down) DSC of a_mZIF-8 exhibing an exothermic transition with onset 282 °C
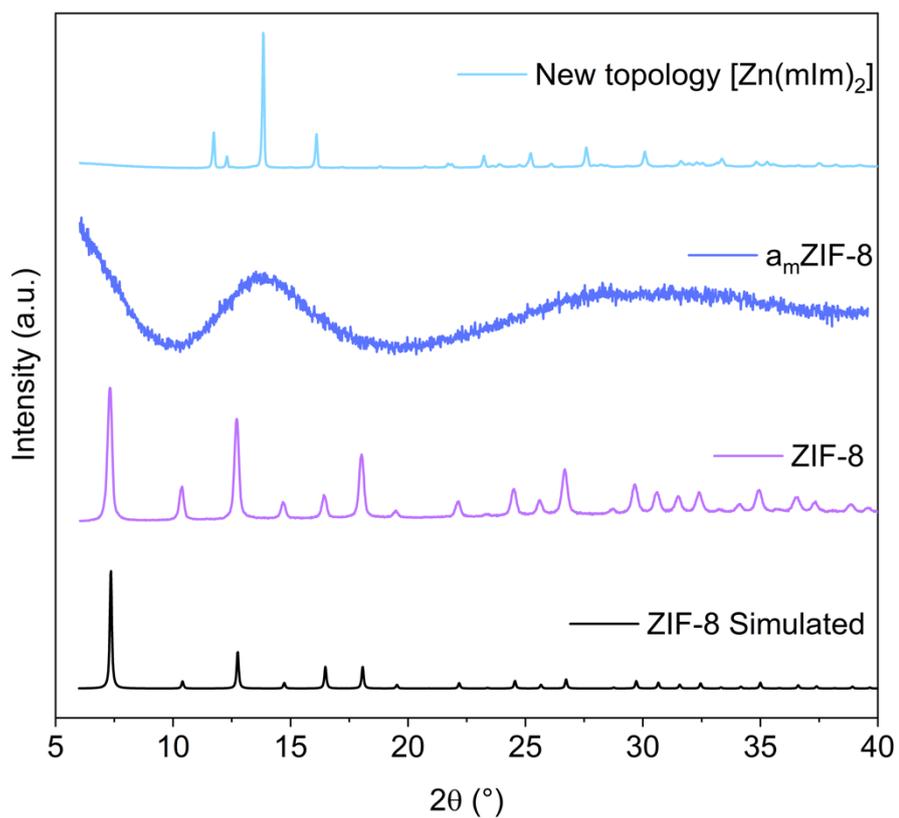
Figure S4: PXRD patterns of simulated ZIF-8, and experimental data from ZIF-8, a_mZIF-8 and the new ZIF-8 phase formed after heating a_mZIF-8 to 400 °C. PXRD collected at Bruker Cu-source diffractometer (λ = 1.5406 Å).

Figure S5: Optical microscopy of ZIF-8, a_mZIF-8 and **qtz**-[Zn(mIm)$_2$].
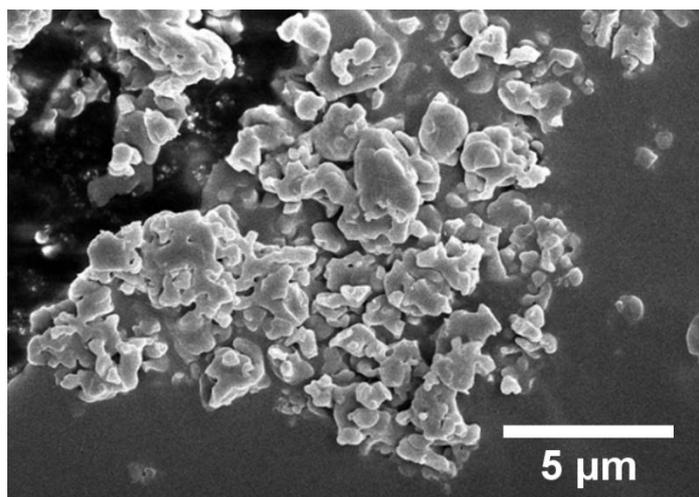
Figure S6: SEM image of **qtz**-[Zn(mIm)$_2$], showing ~1 µm sized particles.

Structure solution from PXRD data

Unit cell determination.

Unit cell determination was carried out using the Materials Studio Reflex Indexing module for peak selection and interfacing with DICVOL91. The most satisfactory solution was found in the hexagonal system with 30 of 30 peaks found (a = 17.3850(12) Å, c = 24.0948(17) Å, V = 6306.721(3) Å^3, FOM = 11.90). Full pattern profile matching and extraction of the integrated intensities (I_{obs}) was conducted with Jana2006.[2] The background was first refined applying an 8th order Legendre polynomial function. The profile was calculated starting with the unit cell parameters obtained from the indexing process and the space group $P6_122$, which agrees with the systematic absences of the diffraction pattern. The integrated intensities (F^2_{obs}) were extracted by a full pattern decomposition using a Thompson-Cox-Hasting Pseudo-Voigt peak profile. Final refined unit cell parameters and plot are depicted below.

Table S2: Refined unit cell parameters and residuals

a	c	R_p	R_{wp}	GOF
17.3850(12)	24.0948(17)	1.29%	1.87%	0.98
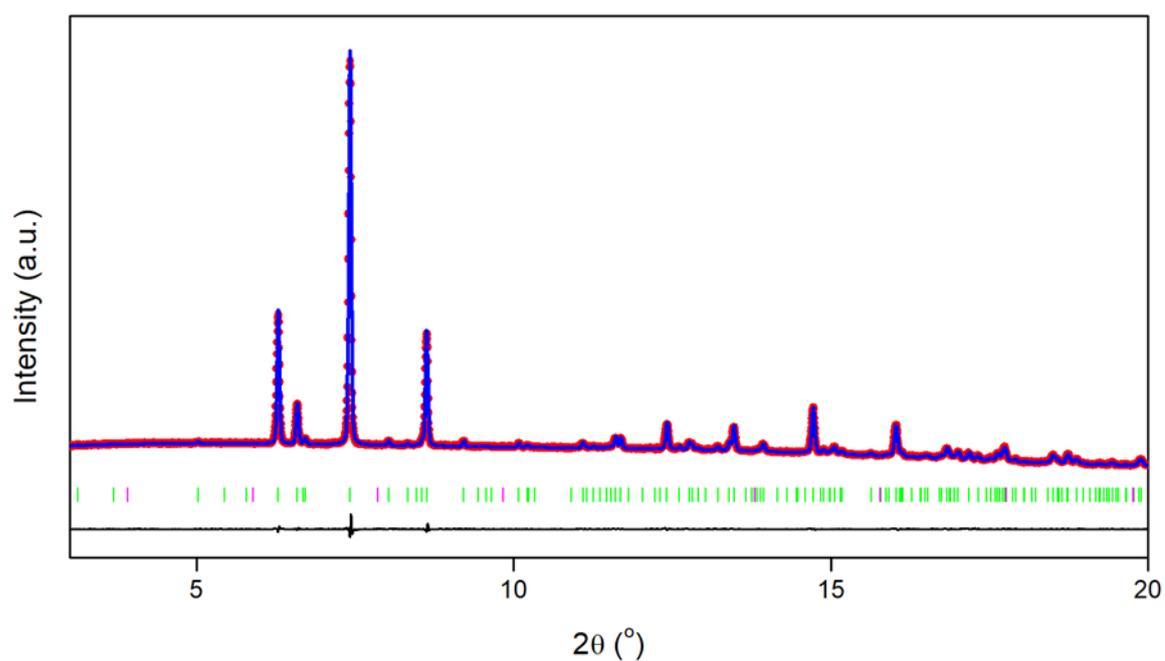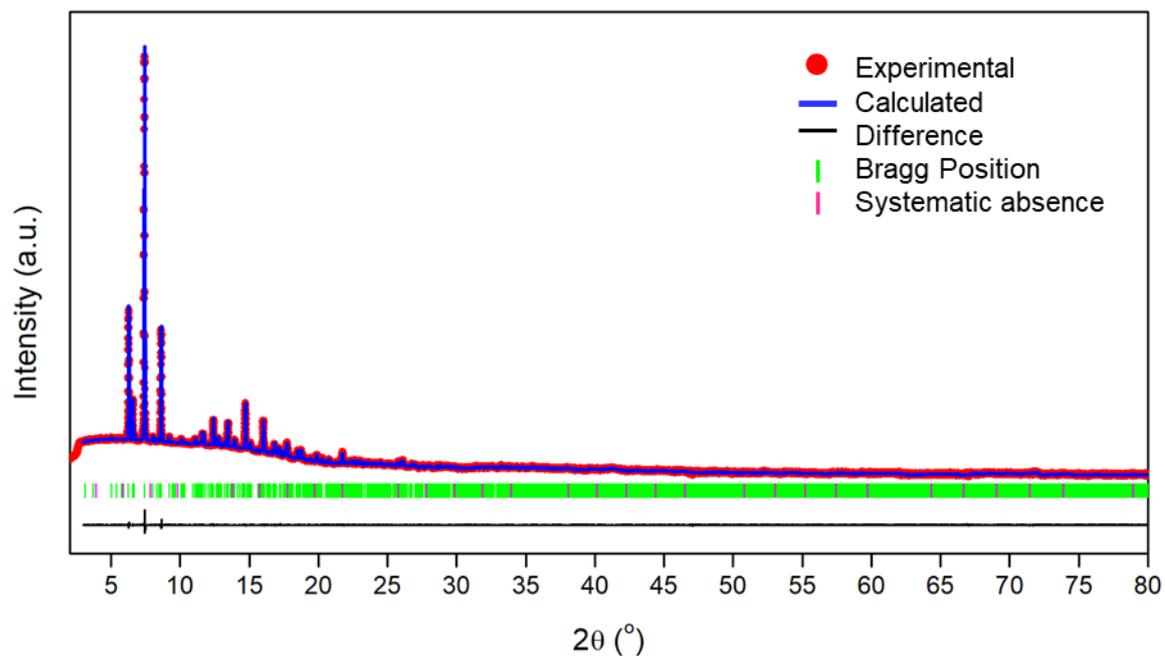
Figure S7: Experimental data (red dots), calculated profile (blue line), difference plot [(I_{obs}–I_{calc})] (black line) and Bragg positions (green ticks) for the Pawley refinement of experimental diffraction data with the obtained cell: a = 17.3850(12) Å, c = 24.0948(17) Å, space group: $P6_122$ (top) all data; detail of the refinement between 3-20° 2θ (bottom). Experimental XRD pattern was collected at Diamond Light Source, I-11 beamline, λ = 0. 0.82697 Å.

Electron density calculation

Electron density maps were calculated using Superflip.[3] The calculation of electron density was performed by extracting the indexed integrated intensities obtained from the Pawley fit, assuming a composition of $Zn_2C_{16}H_{20}N_8$ for the asymmetric unit. The electron density map resulted in a valid density map with $P6_122$ as the proposed space group. The electron density maps were visualised, and the images produced with the Chimera software.
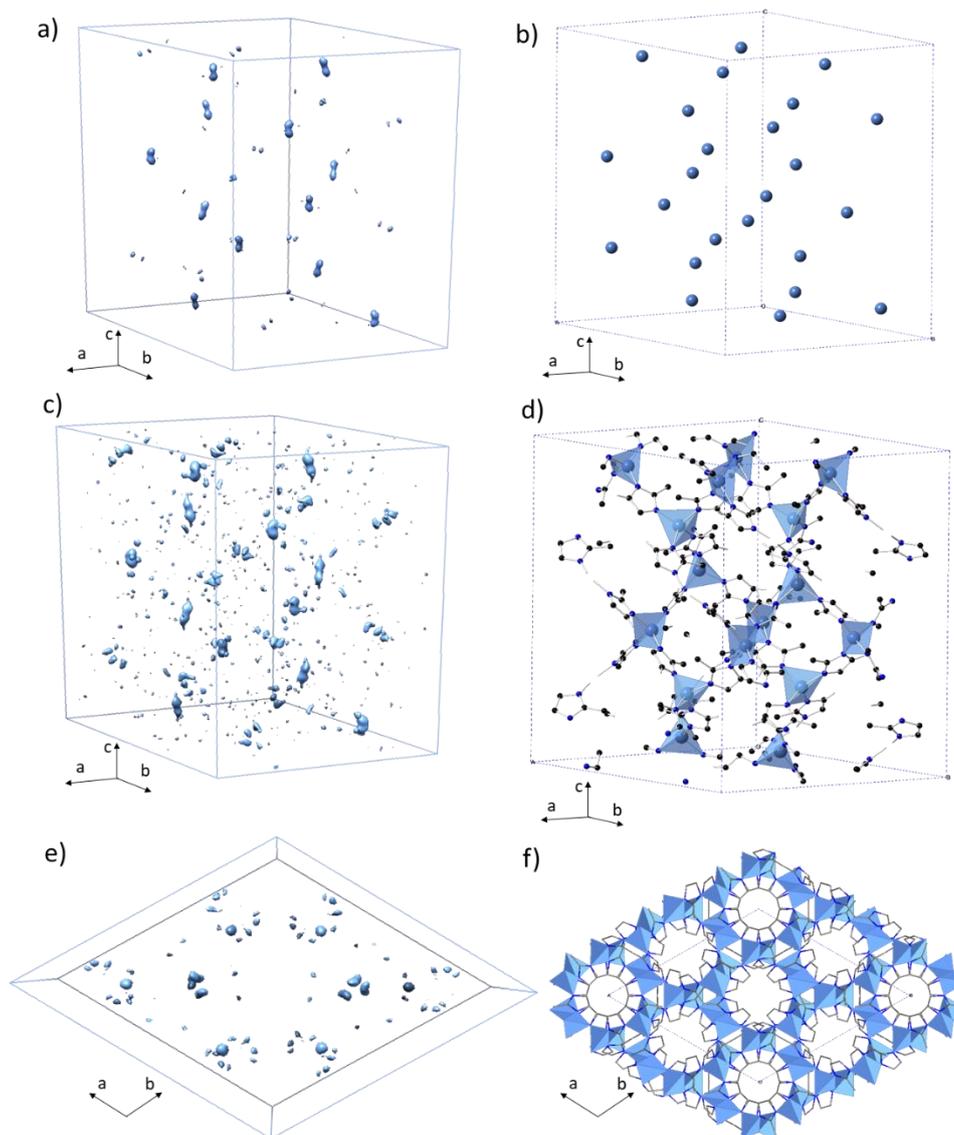
Figure S8: Electron density maps and structure. a) Depiction of the 3D electron density map of most intense peaks in the unit cell; b) Depiction of the Zn atoms obtained from EDMA (Electron Density Map Analysis); c) 3D electron density map decreasing the minimum electron density intensity in the unit cell compared to a). Zn atoms are still visible whilst light atoms (C and N) are difficult to assign through EDMA; d) Model prepared including mIm linker in the structure as rigid bodies; e) 3D electron density map in the view down the *c* axis; f) Model prepared including mIm linker in the structure as rigid bodies in the plane *ab.*

Rietveld refinement

Rietveld refinement was performed using Materials Studio Reflex Refinement module, using synchrotron data from $2\theta = 3\,° - 40\,°$. The profile obtained from Pawley fitting was used as starting set to give the initial parameters for refinement. The profile used was a Pseudo-Voigt function, with a 20th order of polynomial as background. Unit cell parameters, zero-shift correction, and strains were refined observing convergent refinements. Zn atomic coordinates were obtained using EDMA software (Electron Density Map Analysis).[4] Atomic positions were refined constraining the mIm unit as a rigid body. Finally, anisotropic thermal parameters were refined. Hydrogen atoms of the mIm ring were calculated and then included in the refinements. Hydrogens present in C6 were split with 0.5 partial occupancy. Some of the crystallographic parameters obtained from the Rietveld refinement are summarised in Table S3.
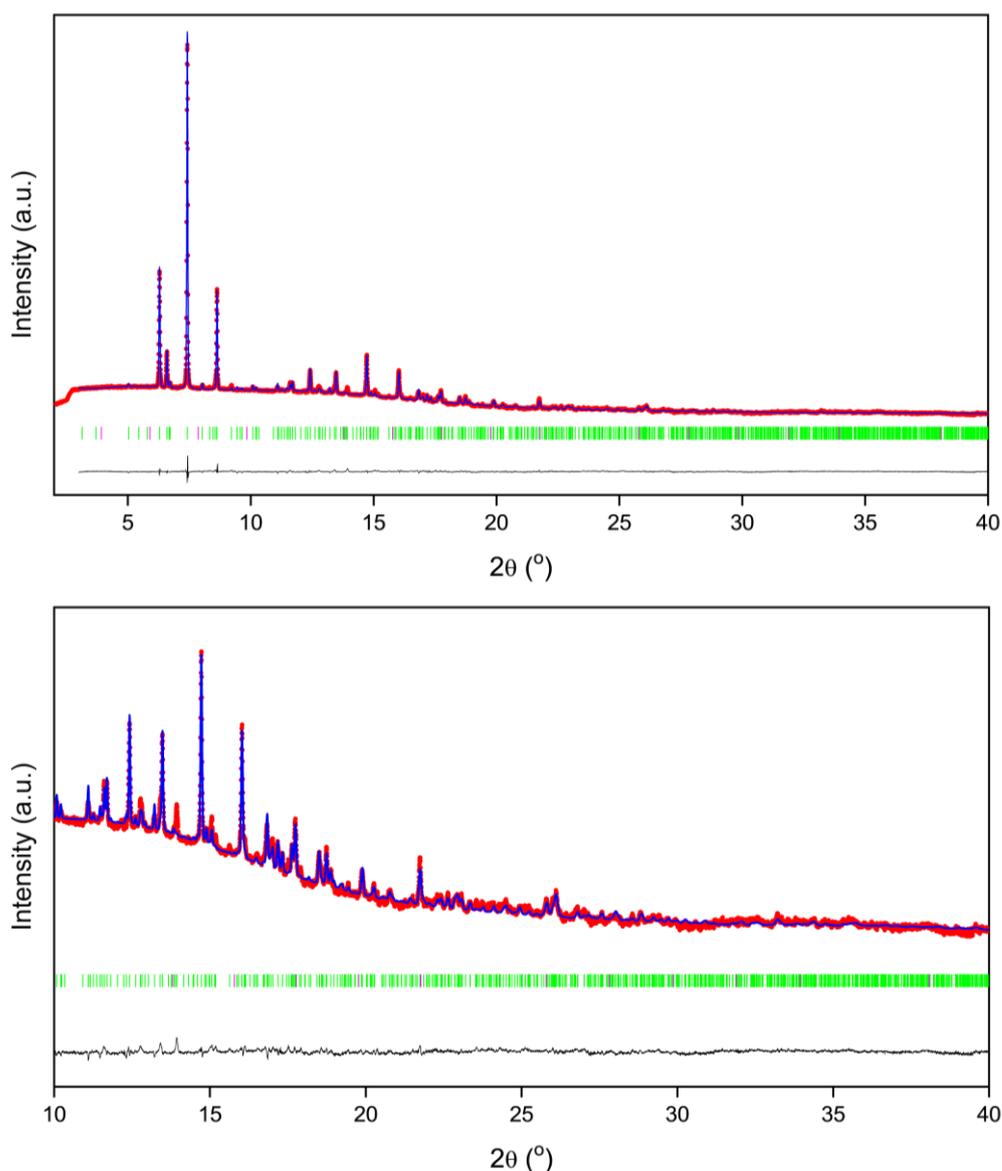
Figure S9: Experimental (red dots), calculated (blue line), difference plot [(I_{obs}–I_{calc})] (black line) and Bragg positions (green ticks, bottom panel) for the Rietveld refinement of experimental diffraction data with the obtained cell: a = 17.36211(21) Å, c = 24.07109(63) Å, space group: $P6_122$. The experimental XRD pattern was collected at Diamond Light Source, I-11 beamline, λ = 0.82697 Å. The top and bottom panels show the 2θ range from 2-40° and 10-40° respectively.

Table S3: Crystallographic data and Rietveld refinement of **qtz**-[Zn(mIm)$_2$]

Compound	qtz-[Zn(mIm)$_2$]
CCDC	2149756
Empirical Formula	C16 H20 N8 Zn2
Molecular Weight, g/mol	455.18
Crystal System	Hexagonal
Space Group	$P6_1 22$
a, Å	17.36211(21)
b, Å	17.36211(21)
c, Å	24.07109(63)
α, °	90
β, °	90
γ, °	120
$V/\text{Å}^3$	6283.925(12)
Z	12
Temperature, K	298
Wavelength, Å	0.82697
2Θ range, °	3-40
Density, g cm^{-3}	1.443
Mu, mm^{-1}	3.465
F000	2784.0
R_p, %	2.20
R_{wp}, %	2.95

Topology
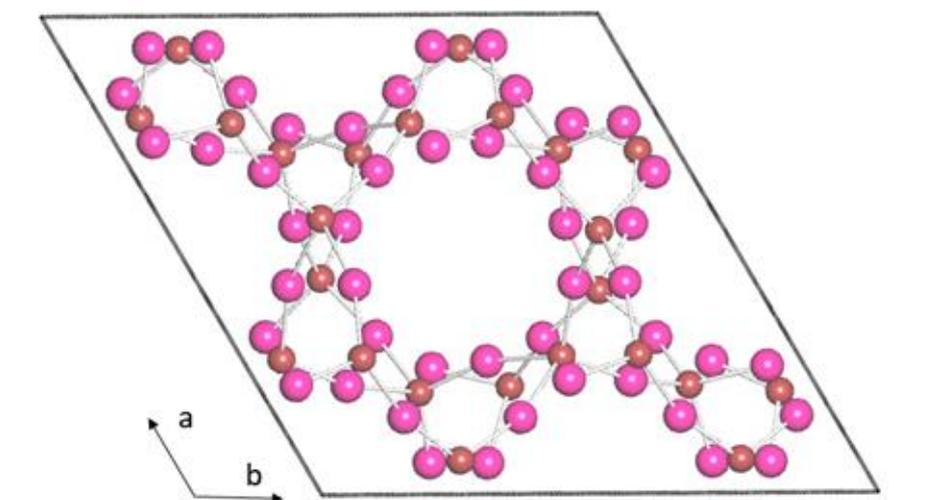
Figure S10: Simplified net of **qtz**-[Zn(mIm)$_2$]. Zn (red), mIm (pink).
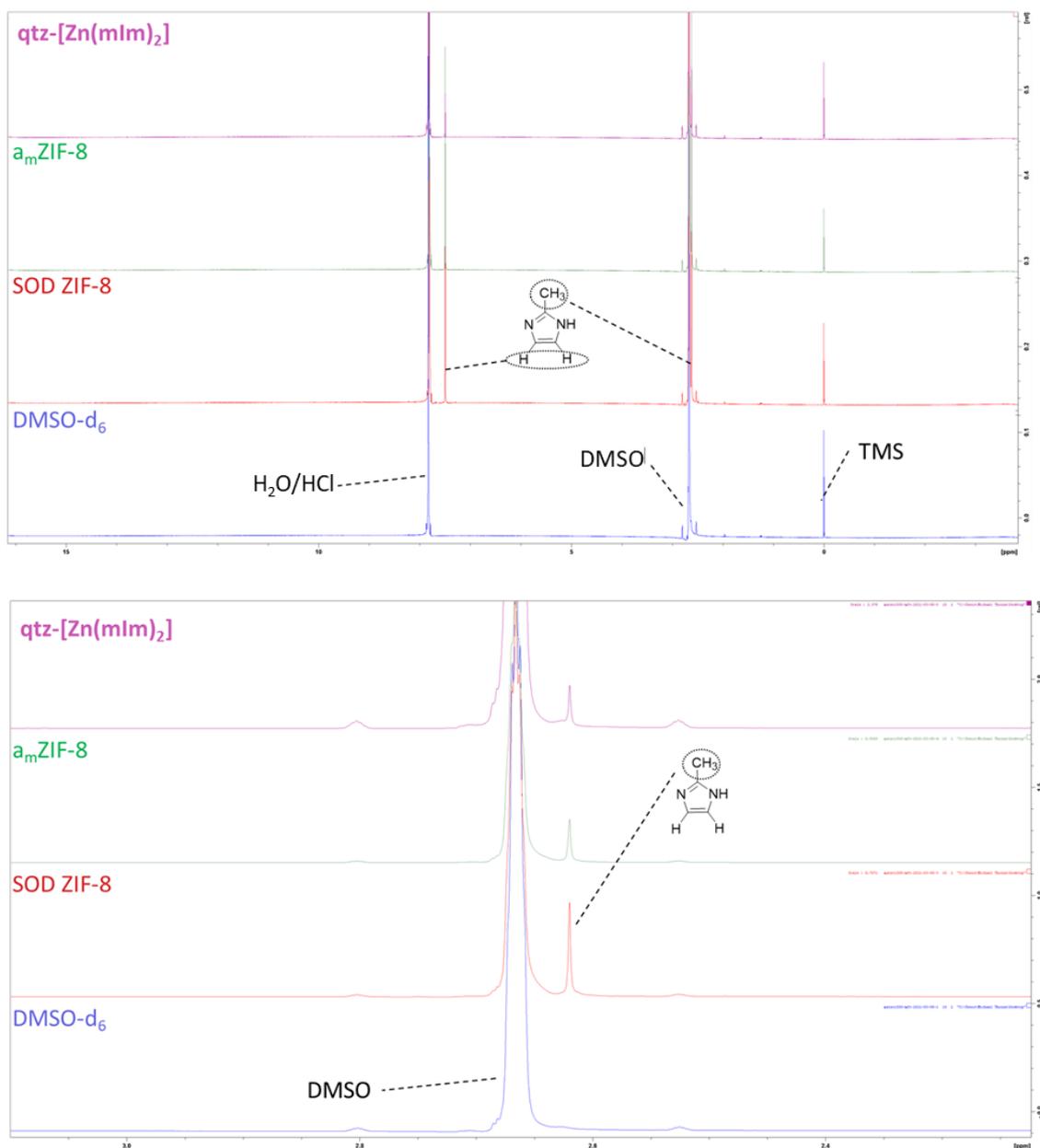
Figure S11: ^{1}H NMR of ZIF-8, amZIF-8 and qtz-[Zn(mIm)$_2$] showing retention of the 2-methylimidazole linker upon amorphisation and subsequent heat treatment to form qtz-[Zn(mIm)$_2$].

Table S4: CHN microanalysis of ZIF-8, a_mZIF-8 and **qtz**-[Zn(mIm)$_2$].

Material	C (%)	H (%)	N (%)
ZIF-8	41.2	4.3	23.8
a_mZIF-8	40.8	4.3	23.4
qtz-[Zn(mIm)$_2$]	40.4	3.9	23.0
Predicted	42.2	4.4	24.6
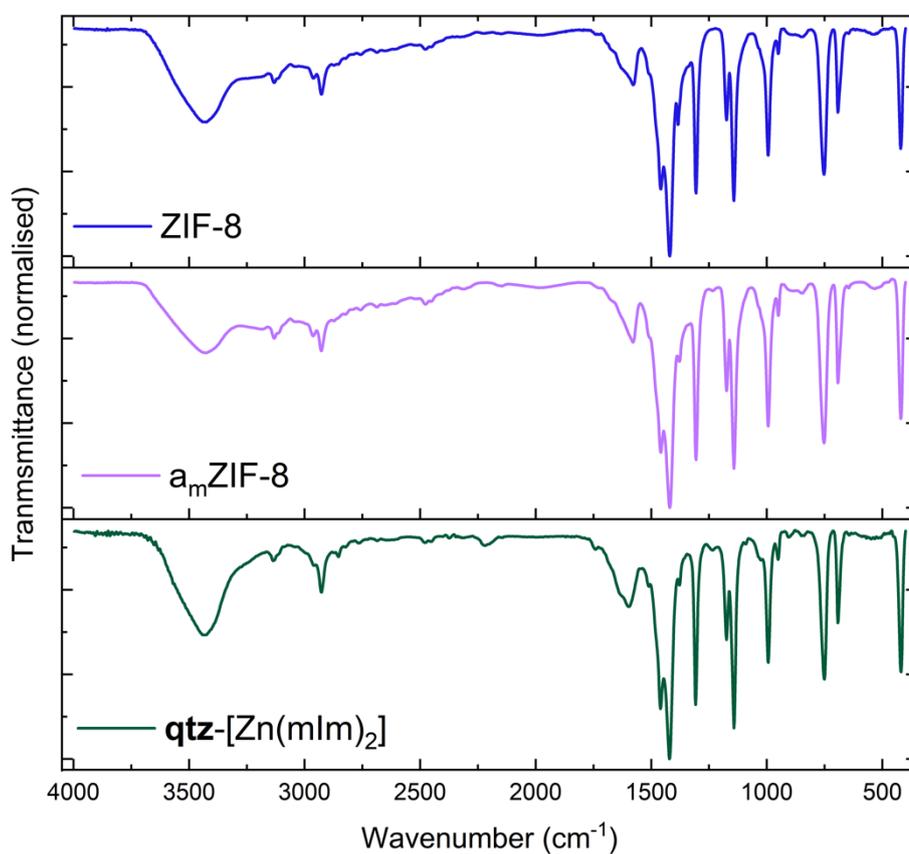
Figure S12: FTIR of ZIF-8, a_mZIF-8 and **qtz**-[Zn(mIm)$_2$]. Spectra were normalised using an internal standard. Namely the absorbance at 1421 cm^{-1}.
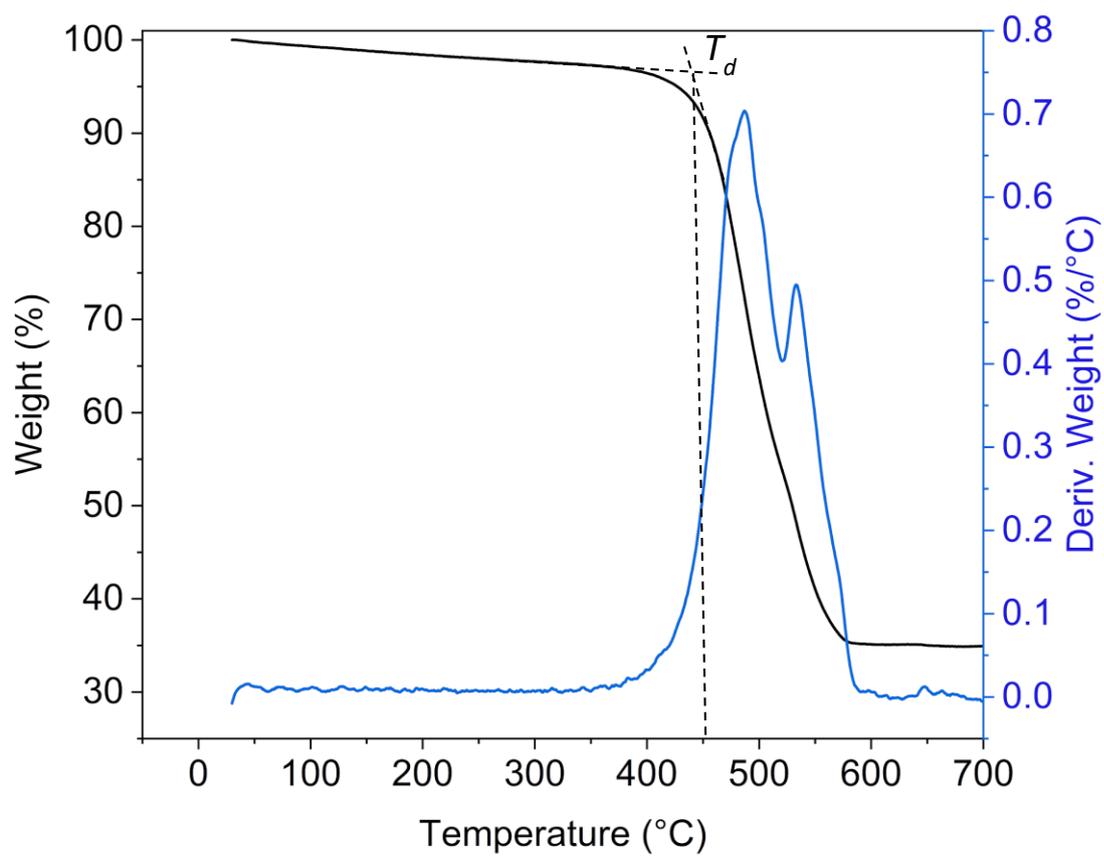
Figure S13: TGA of **qtz**-[Zn(mIm)$_2$] performed at 10 °C min^{-1} under an argon atmosphere showing major onset of decomposition at 452 °C.
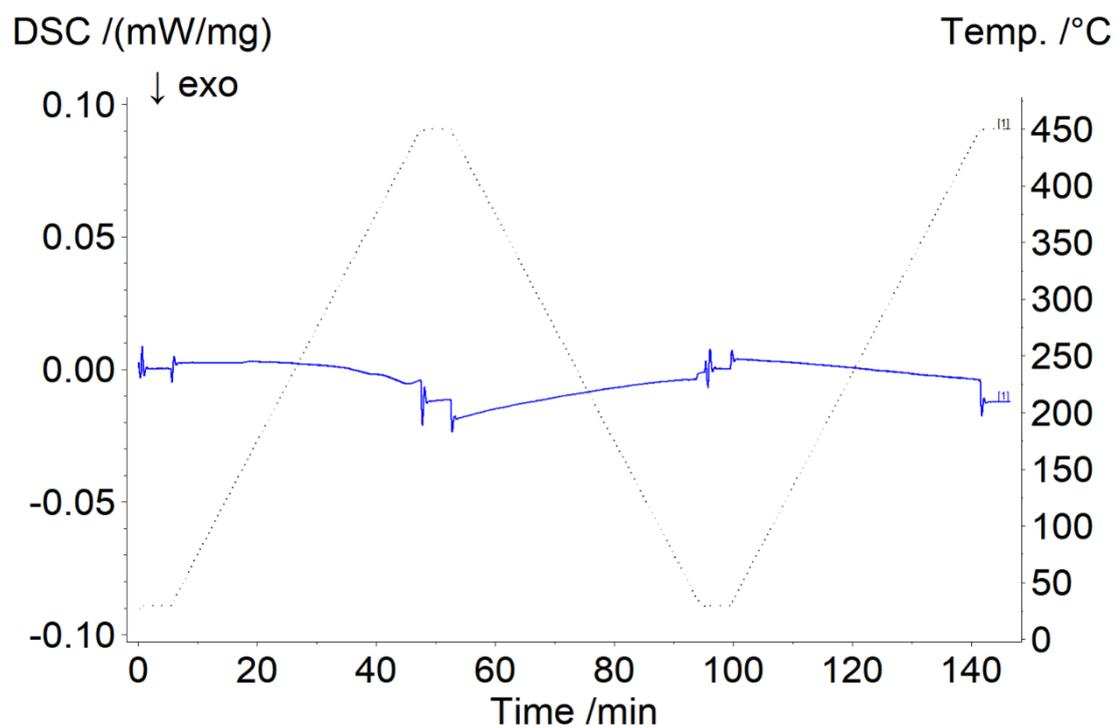
Figure S14: DSC scan of **qtz**-[Zn(mIm)$_2$] to 450 °C, followed by cooling to 40 °C and reheating to 450 °C performed at 10 °C min^{-1} under an argon atmosphere, with 5-minute isothermal segments between each ramping segment. This shows no further thermal events prior to decomposition.
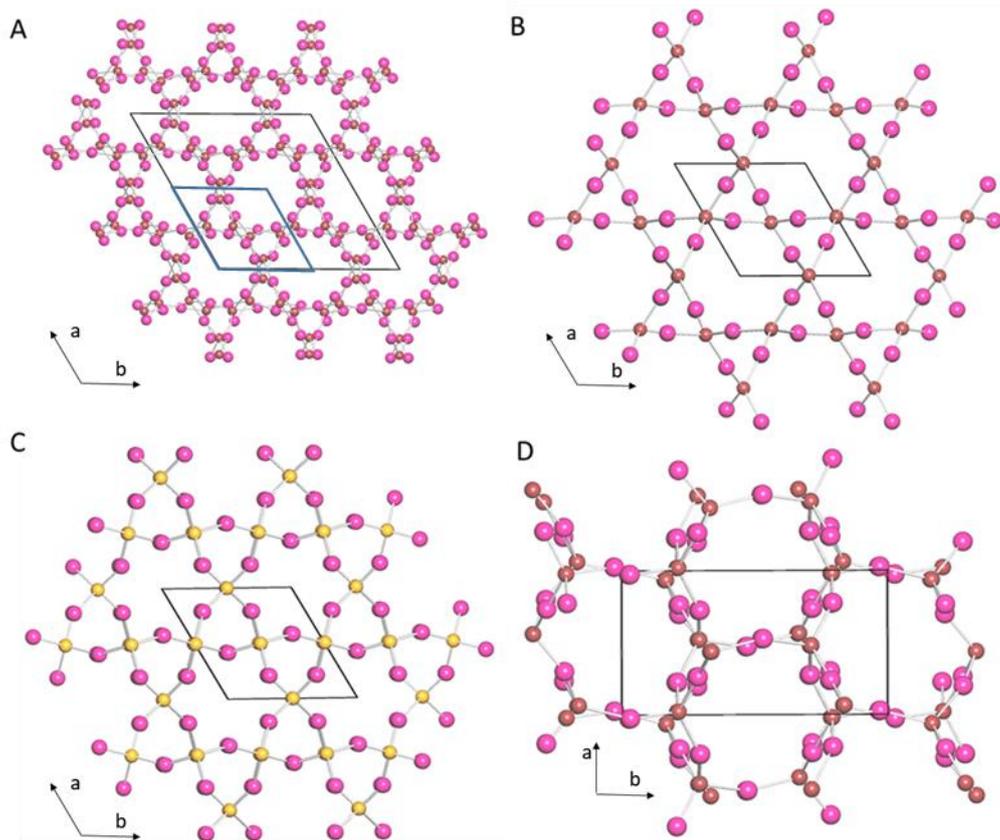
Figure S15: Comparison between topology of different structures: A) **qtz**-[Zn(mIm)$_2$], B) **qtz**- [Zn(eIm)$_2$], C) **qtz**-[Fe(mIm)$_2$] and D) **dia**-[Zn(mIm)$_2$]. The blue diamond in A) shows the unit cell with the equivalent *a* parameter in B) and C). Zn and Fe cations are depicted in yellow and red, respectively. Imidazolates appear as pink spheres.

Structural description of qtz-[Zn(mIm)$_2$]

The Zn atoms are in the special positions $\left(x, 2x, \frac{1}{4}\right)$, $\left(\bar{x}, 2\bar{x}, \frac{3}{4}\right)$, $\left(\bar{x}, x, \frac{5}{12}\right)$. The mIm linker is situated on general positions and bonded to two metal centres. Each Zn atom is surrounded by 4 nitrogen atoms from different ligand molecules in a distorted tetrahedral coordination, with two equivalent distances for Zn1 and Zn2 and four unequivalent distances for Zn3 (**Table S5**). Imidazolate groups are bonding to Zn atoms related by a positive and negative translational 6_1 axis, this generates a double helix of Zn-tetrahedra (**Figure S17**).

Table S5. Zn-N distances for **qtz**-[Zn(mIm)$_2$] structure

Zn1		Zn2		Zn3	
N5_1	2.1123(2) Å	N5_3	2.0594(2) Å	N2_1	1.9432(2) Å
N5_2	1.8878(2) Å	N2_2	1.8170(2) Å	N2_3	2.0747(2) Å
N5_1	2.1123(2) Å	N5_3	2.0594(2) Å	N2_4	2.1694(2) Å
N5_2	1.8878(2) Å	N2_2	1.8170(2) Å	N5_4	1.8134(2) Å
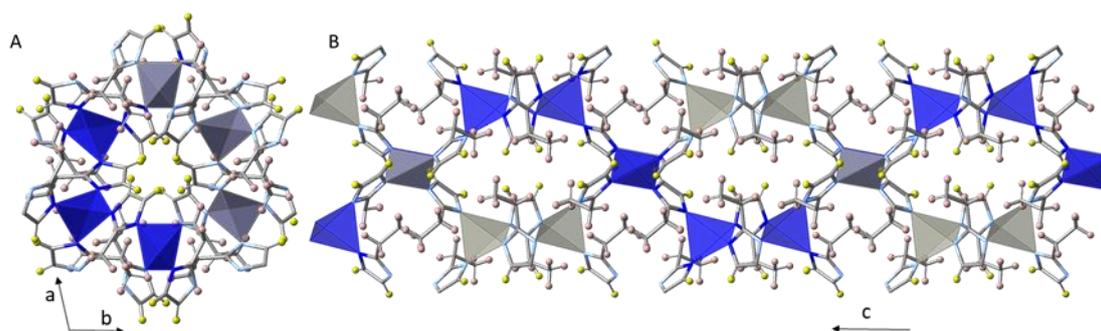
Figure S16: A) **qtz**-[Zn(eIm)$_2$] double helix along c axis. B) Double helix along a axis. Zn tetrahedra from one helix are depicted in blue and the other in grey. Hydrogens from methyl groups are depicted in pale pink and hydrogens from imidazolate are depicted in yellow.[5]
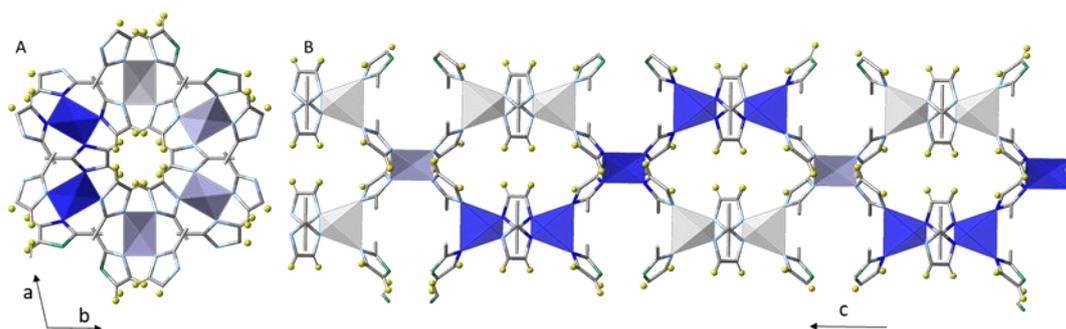
Figure S17: **qtz**-[Fe(mIm)$_2$] structure. A) along c, B) along the a axis. Hydrogens from imidazolate framework are positioned to the interior of the double helix.[6]
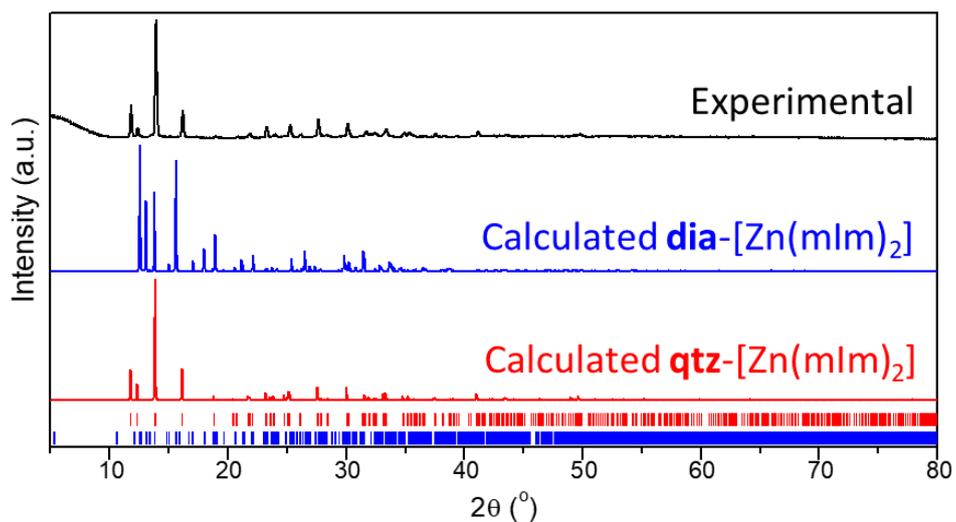
Figure S18: Comparison simulated PXRD (λ = 1.5406 Å) simulated patterns from **dia**-[Zn(mIm)$_2$], and **qtz**-[Zn(mIm)$_2$] structures with the experimental. **dia**-[Zn(mIm)$_2$] calculated pattern was obtained from Ref [7].
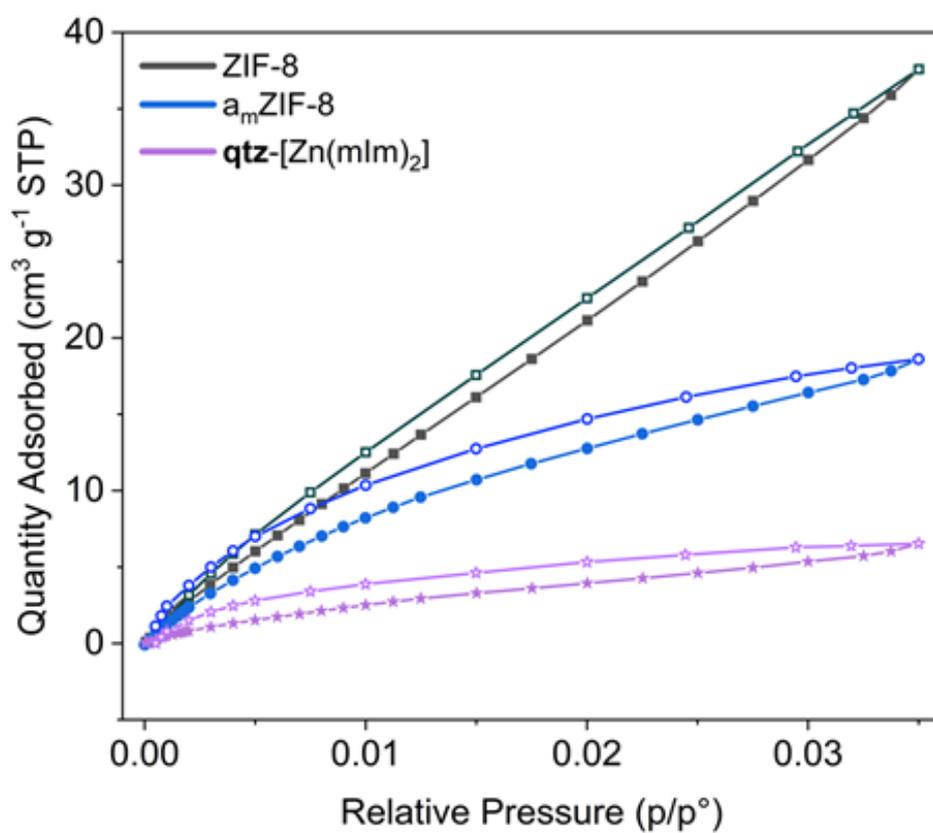
Figure S19: CO_2 adsorption-desorption isotherms collected at 0 °C for: ZOF-8 SOD (grey squares), a$_m$ZIF-8 (blue circles) and qtz-[Zn(mIm)$_2$] (pink stars). Adsorption (closed shapes) and desorption (open shapes).

Figure S20: Photograph of methylene blue solutions after 48 hours of stirring with ZIF-8, a$_m$ZIF-8 and **qtz**-[Zn(mIm)$_2$], followed by filtering. The starting stock solution is presented for reference.
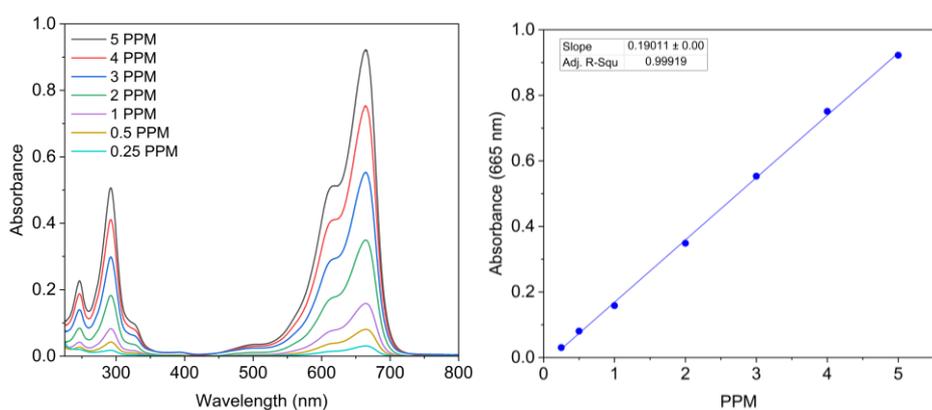
Figure S21: UV-*VIS* spectra of variable MB concentrations in water used for calibration curve and the determined calibration curve of UV-*VIS* absorption data for MB in water.

Table S6: Absorbances of aqueous MB solutions after dye extraction using various ZIFs, with determined remaining PPM of dye and the total dye adsorbed from the starting stock solution of 5 ppm MB.

Material	Absorbance (665 nm)	Dye remaining (PPM)	Dye adsorbed (%)
ZIF-8	0.068	0.359	92.82
a$_m$ZIF-8	0.190	0.999	80.02
qtz-[Zn(mIm)$_2$]	0.541	2.845	43.10
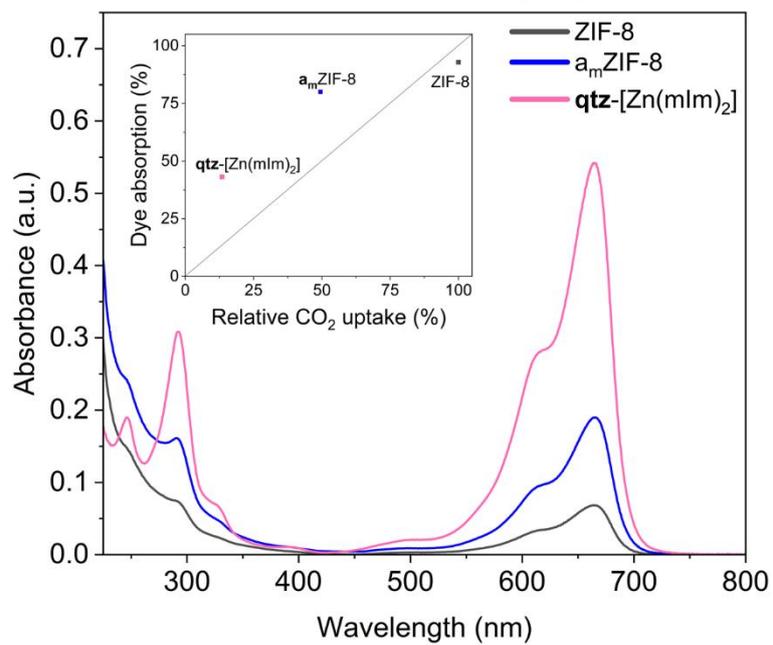
Figure S22: Methylene blue (MB) absorbance spectra for ZIF dye absorption experiments, showing clear differences in the MB absorption peaks for each different ZIF topology. Inset: Relative CO_2 uptake, *vs.* dye absorption showing a strong divergence from a linear relationship between CO_2 uptake and dye absorbance.

Acknowledgements

References

1   K. S. Park, Z. Ni, A. P. Côté, J. Y. Choi, R. Huang, F. J. Uribe-Romo, H. K. Chae, M. O'Keeffe and O. M. Yaghi, *Proc. Natl. Acad. Sci.*, 2006, **103**, 10186–10191.

2   V. Petříček, M. Dušek and L. Palatinus, *Zeitschrift für Krist. - Cryst. Mater.*, 2014, **229**, 345–352.

3   L. Palatinus and G. Chapuis, *J. Appl. Crystallogr.*, 2007, **40**, 786–790.

4   L. Palatinus, S. J. Prathapa and S. van Smaalen, *J. Appl. Crystallogr.*, 2012, **45**, 575–580.

5   Z. Akimbekov, A. D. Katsenis, G. P. Nagabhushana, G. Ayoub, M. Arhangelskis, A. J. Morris, T. Friščić and A. Navrotsky, *J. Am. Chem. Soc.*, 2017, **139**, 7952–7957.

6   A. L. Spek, A. J. M. Duisenberg and M. C. Feiters, *Acta Crystallogr. Sect. C Cryst. Struct. Commun.*, 1983, **39**, 1212–1214.

7   Q. Shi, Z. Chen, Z. Song, J. Li and J. Dong, *Angew. Chemie Int. Ed.*, 2011, **50**, 672–675.